# *In Situ* Formation of Nanocomposites Based on Polyethylene and Silica Nanospheres

**Paula Zapata,[1] Raúl Quijada,[1] Rosario Benavente[2]**

[1]*Departamento de Ingeniería Química y Biotecnología, Facultad de Ciencias Físicas y Matemáticas, Universidad de Chile and the Centro para la Investigación Interdisciplinaria Avanzada en Ciencias de los Materiales (CIMAT), Blanco Encalada 2008, piso zócalo, Santiago, Chile*
[2]*Instituto de Ciencia y Tecnología de Polímeros (CSIC), Juan de la Cierva 3, 28006. Madrid, Spain*

Received 16 February 2010; accepted 26 May 2010
DOI 10.1002/app.32888
Published online 23 August 2010 in Wiley Online Library (wileyonlinelibrary.com).

**ABSTRACT:** Polyethylene nanocomposites containing silica nanospheres, synthesized by the sol–gel method, were produced via *in situ* polymerization. The silica nanospheres were added together with the catalytic system [metallocene catalyst and methylaluminoxane (MAO) as cocatalyst] directly to the reactor and used for the polymerization of ethylene. The polymerization activity increased slightly in the presence of 1 wt % silica nanospheres in comparison to the homogeneous polymerization sans filler. The Young's modulus of the nanocomposites increased 19–25% without a significant decrease in the elongation at break with respect to the neat polyethylene. The polymer particle morphology was also significantly improved with the incorporation of silica nanospheres. © 2010 Wiley Periodicals, Inc. J Appl Polym Sci 119: 1771–1780, 2011

**Key words:** silica nanospheres; nanocomposites; polyethylene; metallocene catalyst

## INTRODUCTION

Mixing polymers with inorganic materials having at least one dimension in the nanometer range is a useful method to produce new materials called polymer nanocomposites.[1,2] Compared to neat polymers and micro-particulate composites, nanocomposite materials have markedly improved properties, including elastic modulus, mechanical strength, barrier performance, optical transparency, and solvent and heat resistance.[3,4] Furthermore, these improvements are achieved at low loadings of the inorganic component (1–10 wt %) in contrast to conventionally-filled polymers which generally require higher loadings of 25–40 wt % to achieve similar properties. As they require much less inorganic material, nanocomposites retain the low density of the matrix and are more easily processed than conventional composites.[5–7]

The properties of nanocomposites are not only influenced by the kind of filler,[8] but also by the microstructure of the polyolefins and the preparation process.[9] There are three main methods used to produce polymer nanocomposites: (i) melt compounding, (ii) solution blending, and (iii) *in situ* polymerization.[10,11] *In situ* polymerization is perhaps considered the most promising technique to produce polymer nanocomposites as the direct synthesis via polymerization in the presence of the filler enhances the dispersity of the inorganic particles in the polymer matrix and improves the compatibility between the inorganic particles and the polymer.[1]

Metallocenes are an important class of catalysts for ethylene and propylene polymerization due, in part, to the possibility of tailoring the molecular structure of the polymers. Metallocene catalysts activated by methylaluminoxane (MAO) produce polyethylene (PE) with narrow molecular weight distributions and high activities.[12–14] The main disadvantages of metallocene-based polymerizations are the lack of control with respect to polymer particle morphology and reactor fouling when these catalysts are used in homogeneous processes. As the addition of silica particles to polymerization reactions has previously been shown to produce particle replication, the *in situ* production of polyethylene nanocomposites using metallocene catalysts also serves to improve the polymerization behavior and morphology of the final product. Nanoscale, synthetic inorganic materials such as $SiO_2$, $Al_2O_3$, $ZrO_2$, $TiO_2$, and natural layered clays have attracted much attention as filler materials for the preparation of nanocomposites.[10,11,14–17] One important material is nanosilica which can be obtained by the sol–gel method. This method allows for the preparation of silica particles in the nanometer range with morphology control and well-defined pore size distribution.[18]

*Correspondence to:* P. Zapata (paulaandreazapataramirez@yahoo.es).

Contract grant sponsors: CONICYT (FONDAP project 11980002), Ministerio de Ciencia e Innovacion (Project MAT2007-65519-C02-01).

In the literature micrometer range silica particles are generally used to support metallocene catalysts for ethylene polymerization.[19–21] However, the preparation of nanocomposites by *in situ* polymerization using silica nanoparticles both as a support for the metallocene catalyst and as filler has only been discussed in a few research articles.

Linear low-density polyethylene (LLDPE) has been produced using zirconocene/MAO as catalyst with MAO impregnated nano-$SiO_2$ and nano-$ZrO_2$ as the support/filler.[11] The same authors,[10] studied the effect of nanoscale $SiO_2$ particle size on the catalytic activity, polymer morphology, and nano-$SiO_2$ dispersion in the polymer matrix. They found that larger particles (nanometer range) had higher activity. However, no change in the molecular structure of LLDPE was observed. TEM analysis of the composites showed that the nanoscale filler was poorly dispersed due to particle agglomeration. No evaluation of the mechanicals properties of the nanocomposites was reported.

Nano-sized silica particles were used as support for a metallocence/MAO catalyst in ethylene and propylene polymerizations.[14,22] The nanoscale catalyst system showed enhanced ethylene and polypropylene polymerization activities compared to catalyst systems supported on micro-scale filler under identical reaction conditions. As determined by X-ray diffraction (XRD) and density measurements, the crystalline structure of the polymers did not change in the presence of nano-sized silica.

Polyethylene and polypropylene nanocomposites were prepared using nanoparticles such as silica balls (monospheres), calcium carbonate, multiwalled carbon nanotubes (MWCNT), and carbon fibers (CF) pretreated with MAO.[9,23] The presence of the filler materials in these reactions did not significantly change the polymerization activities. The incorporation of MWCNT, carbon fibers, and silica monospheres into the PP led to an increase in the crystallization temperature. It was found that the yield strength and strain-to-failure of syndiotatic polypropylene (sPP) containing 0.6 wt % of MWCNT was higher than that of the neat sPP.

The preparation of nanoparticle supported metallocene catalysts is an extensive one, and requires a great deal of time. In addition, the catalytic activity in heterogeneous polymerizations using micro silica decreases compared to comparable homogeneous systems. This can be due to the silica surface impeding monomer access to the active center, reducing the activity.[24,25] It was thought that an alternative to the heterogeneous system would be to add the silica particles and the catalytic system to the reaction at the same time. In this study, a facile route for the *in situ* preparation of polyethylene nanocomposites using untreated silica nanospheres, synthesized by the sol–gel method, as filler was developed. In this approach the nanospheres are placed in contact with the cocatalyst (MAO) and the metallocene catalyst directly in the reactor. The effect of the silica nanosphere loading on the catalytic activity of the system and on the properties of the resulting polymer nanocomposites was studied. These properties include; molecular weight, thermal properties, mechanical response using uniaxial tensile stress–strain, microhardness measurements, and viscoelastic behavior by means of dynamic–mechanical thermal analysis (DMTA).

## EXPERIMENTAL

### Materials

The metallocene catalyst, bis(*n*-butylcyclopentadienyl) zirconium dichloride ($(n\text{BuCp})_2ZrCl_2$) (Aldrich) was used as the ethylene polymerization catalyst, and MAO (Witco) as cocatalyst. Ethylene was deoxygenated and dried by passage through columns of Cu catalyst (BASF) and activated molecular sieves (13×), respectively. Toluene was purified by refluxing over Na/benzophenone and distilling under nitrogen. All manipulations were carried out in an inert nitrogen atmosphere using standard Schlenk techniques.

Silica nanospheres were synthesized using the sol–gel method as previously reported.[18] The reagents used in the synthesis of the nanoparticles were tetraethyl orthosilicate (TEOS), ($Si(OC_2H_5)_4$), (98%, Aldrich), distilled ethanol (96%), aqueous ammonia ($NH_4OH$, 28%, Merck), and distilled water.

### Preparation of spherical nanoparticles (SN)

Monodisperse spherical $SiO_2$ nanoparticles were prepared by hydrolysis of TEOS using a two-stage mixed semibatch method.[18] In the first stage, two solutions were prepared. Solution 1 was prepared by dissolving 0.5*M* TEOS in 22 mL of ethanol. In Solution 2, aqueous ammonia solution (0.2*M*) was added to 23 mL ethanol and 2 mL of distilled water. Solution 2 was then added dropwise to Solution 1. The resulting mixture was allowed to react for 60 min at 40°C under $N_2$ atmosphere. The second stage of the procedure consisted of preparing Solutions 1 and 2 again and adding them to the reactor containing the solution and particles prepared in the first stage. The solutions were mixed for 60 min at 40°C. The $SiO_2$ particles were separated by centrifugation (10,000 rpm, 20 min) and washed three times with ethanol. The nanoparticles were then calcined for 4 h at 450°C.

### Homogeneous polymerization (neat polyethylene)

Polymerization reactions were carried out in a 600 mL glass reactor (Parr) with mechanical stirrer and temperature controller. Toluene, MAO, and metallocene catalyst solution in toluene were added to the reactor, followed by the addition of ethylene. In each experiment $3 \times 10^{-6}$ mol of metallocene catalyst and 2.6 mL of MAO ([Al]/[Zr] = 1400) were used. The final volume of the solution in the reactor was 240 mL. The polymerization reaction was carried out at 60°C and 2 bar ethylene for 30 min, while stirring at 1000 rpm. The polymerization was terminated by the addition of acidified methanol (10% HCl, 20 mL). The polyethylene product was recovered by filtration, washed with ethanol, distilled water, acetone, and then dried overnight at room temperature. Catalytic activity was expressed as the mass of PE produced per unit time per mol of Zr and per unit pressure (kg $mol^{-1}$ $bar^{-1}$ $h^{-1}$). All polymerization reactions were repeated twice to verify reproducibility.

### Polymerization in the presence of silica nanospheres

The polymerization in the presence of silica nanospheres was carried out using the same reaction conditions as those used in the homogeneous polymerization (neat). The polymerization was carried out by first adding toluene, 2.6 mL of MAO solution and then the silica nanospheres (dispersed in toluene) into the reactor and mixing for 2 min. The silica nanospheres were precontacted with MAO in the reactor to decrease the population of catalyst-deactivating OH groups on the silica surface. The catalyst solution was then added and mixed for 2 min and finally saturated with ethylene. Two different loadings of nanospheres were used (1 and 5 wt % with respect to the weight of the neat polymerization product) to study the effect of the silica loading on catalytic activity as well as on the properties of the polymer obtained.

### Characterization

The characteristic bands of the silica structure were analyzed by diffuse reflectance infrared Fourier transform spectroscopy (DRIFTS) on a Bruker Vector 22 instrument, in the 4000–400 $cm^{-1}$ range with a resolution of 4 $cm^{-1}$ at room temperature.

Molecular weight distributions of the polyethylene products were determined using a Waters Alliance GPC 2000 equipped with three Styragel HT-type columns (HT3, HT5, and HT6E). The 1,2,4-trichlorobenzene was used as solvent, at a flow rate of 1 $cm^3$ $min^{-1}$ and a temperature of 135°C. The columns were calibrated with polystyrene standards.

The melting temperature and enthalpy of fusion of the neat and nanocomposite PE samples were measured by differential scanning calorimetry (DSC) on a TA Instruments DSC 2920. The samples were heated from 25 to 180°C and cooled to 25°C at a rate of 10°C $min^{-1}$; the values were taken from the second heating curve to eliminate any thermal history.

Percent crystallinity was calculated using the enthalpy of fusion of an ideal polyethylene having 100% crystallinity (289 J $g^{-1}$) as reference.[26] Percent crystallinity was calculated using the following equation:[8]

$$\chi(\%) = \frac{\Delta H_c}{(1-\varphi)\cdot \Delta H_0} \times 100$$

Where: $\Delta H_c$ is the melting enthalpy (J $g^{-1}$) of the polymer nanocomposite, $\Delta H_0$ is the value of the enthalpy corresponding to the melting of a 100% crystalline sample (289 J $g^{-1}$), and $\varphi$ is the weight fraction of the filler in the nanocomposite.

The XRD patterns of the silica nanospheres, neat PE, and PE/SN nanocomposites were analyzed by X-ray diffraction (XRD) on a Siemens D5000 diffractometer. Ni-filtered Cu K$\alpha$ radiation was used ($\lambda$ = 0.154 nm).

Polymer particle morphology was observed by SEM on a LEO Gemini 1530 microscope. The morphology of the silica nanospheres and their dispersion in the composites was analyzed by TEM on a JOEL JEM-1200EXII microscope operating at 200 kv. The silica nanospheres specimens were prepared analysis by dispersing them in ethanol, sonicating them for 10 min, then depositing a small drop of the dispersion on a copper grid. Ultra-thin polyethylene nanocomposite specimens with a thickness of $\sim$ 80 nm were cut with glass and diamond blades in an ultra-microtome (Sorvall MT 5000) at −40°C.

The tensile properties of the polymer and composites were determined using an HP model D-500 dynamometer. The materials were molded for 5 min in a HP industrial instruments hydraulic press at 50 bar pressure and 170°C and cooled under pressure with water circulation. Films of about 0.07 mm thickness were obtained. Dumbbell-shaped samples with an effective length of 30 mm and a width of 5 mm were cut from the compression-molded sheets. The samples were tested at a rate of 50 mm $min^{-1}$ at 20°C. Each set of measurements was repeated at least four times.

A Vickers indentor attached to a Leitz microhardness tester was used for microindentation measurements. The microhardness values were calculated according to the relation:

$$\mathrm{MH} = \frac{2\mathrm{sen}\ 68^{\circ} P}{d^2}$$

Where $P$ is the contact load (in $N$) and $d$ is the length of the diagonal of the indentation surface (in mm). All measurements were carried out at 25°C using a load of 0.981$N$.

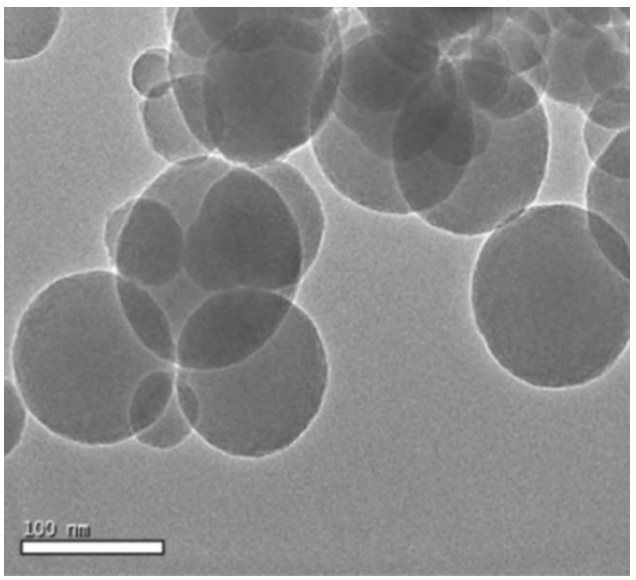


**Figure 1** TEM image of SN obtained by the sol–gel method.

Dynamic mechanical relaxations were measured with a Polymer Laboratories MK II Dynamic mechanical thermal analyzer working in the tensile mode. The storage modulus ($E'$), loss modulus ($E''$), and loss tangent (tan δ) of each sample were obtained as functions of temperature over the range from −140 to 120°C at four frequencies: 1, 3, 10, and 30 Hz, and at a heating rate of 1.5°C $min^{-1}$. Strips of ~ 2.2-mm wide and 15-mm long were cut from the sheets. The apparent activation energy values were calculated from an Arrhenius-type equation, using an accuracy of 1°C in the temperature assignment of loss modulus maxima.

## RESULTS AND DISCUSSION

### Characterization of silica nanospheres (SN)

It can be observed from the TEM micrographs in Figure 1 that the $SiO_2$ particles prepared are spherical, with diameters of about 80–100 nm.

The typical DRIFT signals for silica particles synthesized by the sol–gel method are shown in Figure 2.[7] Bands characteristic of $SiO_2$ are observed: Si—OH at 3745 $cm^{-1}$, attributed to isolated surface OH groups, with a broad band at 3372 $cm^{-1}$, which corresponds to OH groups disturbed by hydrogen bonding due to the presence of adsorbed water.[19] The band at 1632 $cm^{-1}$ is also attributed to presence of the OH groups of water. The bands at 1300 and 1000 $cm^{-1}$ correspond to the intense peaks of Si—O stretching[27] and to the characteristic Si—OH bending peaks of the vibration of the silica structure, respectively.[28]

### Catalytic activity of ethylene polymerization in the presence of silica nanospheres

The polymerization results and polymer properties (molecular weight, melting temperature, and crystallinity) of the synthesized polyethylenes with and without silica nanospheres are shown in Table I. In general, reactions which used silica nanospheres behaved similarly to the homogeneous reaction. When 1 wt % of silica nanospheres was used a slight increase in catalytic activity was obtained in comparison to the polymerizations and nanospheres. Increasing the loading to 5 wt % of silica nanospheres, however, produced a slight decrease in catalytic activity compared to the polymerization with 1 wt % of nanospheres. After thermal treatment (450°C) the silica nanoparticles mainly present isolated single and to a lesser extent geminal hydroxyl groups. The presence of these hydroxyl groups is known to deactivate metallocene catalysts.[29] The OH groups on the silica surface can interact with the metallocene catalyst and eliminate chlorine groups from the metallocene producing an inactive species.[20] Mixing the silica spheres in the reactor with MAO prior to polymerization reduces the surface concentration of these OH groups, and generates sites at which the catalyst can interact. As the OH groups are isolated on the surface, the 450°C pretreatment condenses any adjacent hydroxyls, the resulting MAO capped sites will isolated as well. This creates a minimum amount of spacing between catalysts on the silica surface, and is termed the "spacer effect." This spacing prevents catalyst–catalyst interactions, and as such reduces or even eliminates bimolecular deactivation. At lower filler content (1 wt % of nanospheres), the spacer effect of the spheres seems to favor the catalytic activity.[24] However, when the loading of silica is increased to 5 wt %, the corresponding increase in OH groups (the MAO concentration was maintained constant in the

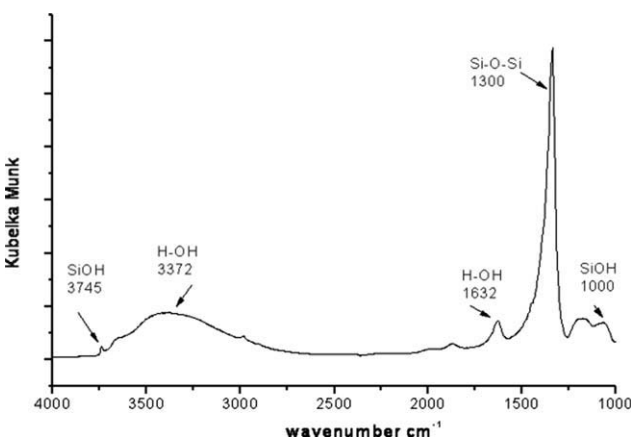


**Figure 2** DRIFT spectrum of SN obtained by the sol–gel method.

**TABLE I**
**Results of Ethylene Polymerizations Using Silica Nanospheres as Filler**

| Process | Silica nanospheres (g) | Silica nanospheres content (wt %) | Catalytic activity (kg mol$^{-1}$ Zr$^{-1}$ h$^{-1}$ bar$^{-1}$) | $M_w$ (kg mol$^{-1}$) | $M_w/M_n$ | $T_m$ (°C) | χ (%) |
|---|---|---|---|---|---|---|---|
| Metallocene Neat PE | 0 | 0 | 3900 | 190 | 2.14 | 139 | 67 |
| Metallocene + | 0.11 | 1 | 4600 | 182 | 2.00 | 137 | 74 |
| silica nanospheres | 0.55 | 5 | 4100 | 250 | 1.81 | 137 | 75 |

PE: polyethylene; $M_w$: molecular weight; PDI : $M_w/M_n$: polydispersity, $T_m$: melting temperature, χ: percent crystallinity. Polymerization conditions: mol Zr: $3 \times 10^{-6}$; Al/Zr: 1400; polymerization temperature: 60°C. Pressure: 2 bar; reaction time: 30 min.

polymerizations) could deactivate the catalytic system counterbalancing the aforementioned spacer effect.

The melting temperature of the nanocomposites did not significantly change compared to the neat PE, indicating the formation of linear polyethylene. The molecular weight of the polymer increased slightly when 5 wt % of silica nanospheres was used. This could be due to the fact that the nanoparticles do not permit bimolecular reactions between two metallocene centers, hindering the β-hydrogen transfer, which would result in longer growth of the polymer chain. This may be associated with a decrease of termination or transfer reactions during polymerization.[19] The presence of silica nanospheres may hinder β-hydrogen transfer, resulting in greater growth of PE (higher molecular weight). However, it is important to mention that the increase in molecular weight could also be due to free trimethylaluminum in the MAO which has been reported to prevent the bimolecular deactivation of metallocene catalysts.[30] The polydispersity (PDI) of ~ 2 for the polymers obtained are typical of metallocene catalysts because they are single site catalysts and have identical active centers.[31] Some authors[19,20,24,32], have reported that when metallocene catalysts are supported on silica for ethylene polymerization the catalytic activity decreased in comparison with homogeneous systems. It has also been reported that the polymerization activity and final properties of the polymers (molecular weight distribution and morphology) depend on the nature of support, method and time used in anchoring the metallocene catalyst.[33] In addition, the molecular weight of polymers produced in supported systems increases in comparison with neat polymers because β-hydrogen transfer is hindered in supported systems.[19] This work did not require long preparation times or troublesome procedures to obtain the system, in addition, the catalytic activity is comparable with the homogenous polymerization and the molecular weight of polymer increases slightly.

The slight increase in the percent crystallinity of the nanocomposites compared to the neat polymer can be attributed to the silica nanoparticles acting as nucleating agents in the crystallization of the polymer, thereby increasing the number of crystalline regions.[6,34] This higher crystallinity could be also related to the increase in molecular weight as well a smaller crystal size.[35] The crystallization curves of neat PE and PE nanocomposites obtained in the presence of 1 and 5 wt % of silica nanospheres are shown in Figure 3. The crystallization temperatures were similar, ~ 118°C; however the shape of the exothermic crystallization peak for neat PE is broader than that of the nanocomposites. It seems that the presence of silica nanoparticles leads to a narrower distribution of crystal sizes.

### Characterization of the nanocomposites

The XRD patterns of the silica nanospheres (SN), neat PE, and PE/SN nanocomposites (1 and 5 wt %) are shown in Figure 4. The XRD pattern of the SN has the characteristic signals of amorphous silica. The XRD pattern of PE show two characteristic peaks at $2\theta = 21.8°$ and 24.3° corresponding to the (110) and (200) planes of the orthorhombic

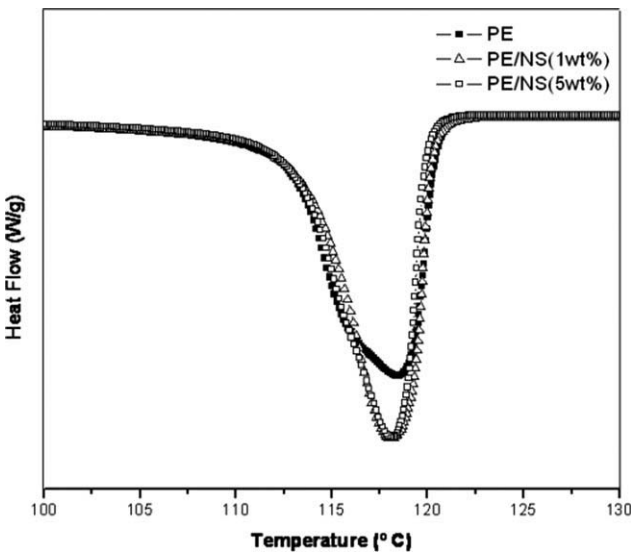


**Figure 3** DSC crystallization curves of neat polyethylene (PE) and nanocomposites with 1 and 5 wt % of silica nanospheres.

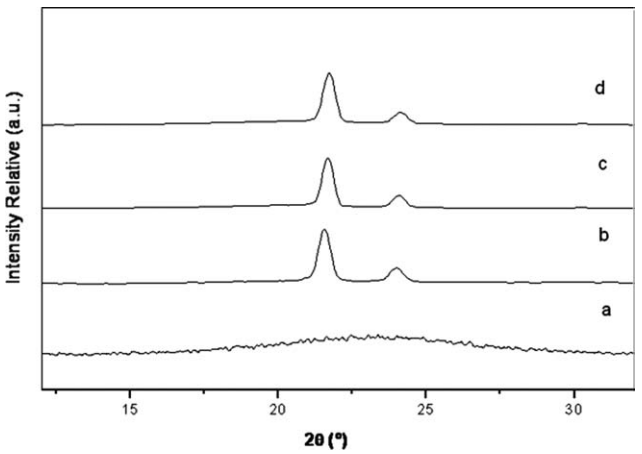


**Figure 4** XRD patterns of (a) SN, (b) neat PE, (c) PE/SN (1 wt %) nanocomposite and (d) PE/SN (5 wt %) nanocomposite.

crystalline form of PE.[14,36] Analysis of the PE/SN nanocomposite XRD pattern shows that incorporation of SN into the PE matrix does not change the intensity or the width of the (110) and (200) diffractions, [Fig. 3(d)], indicating that the polymer retains its crystalline structure.

The materials were analyzed by SEM to compare the morphology of neat PE with that of the 1 wt % PE/SN nanocomposite, Figure 5. The neat polymer exhibits a compact morphology, while the particles of the nanocomposite appear less aggregated. Visual inspection of these polymer products shows that neat PE consists of fiber-like particles whereas the nanocomposites are clearly more powdery products.

Therefore, ethylene polymerization in the presence of silica nanoparticles has a favorable effect on the morphology of the PE product. Similar behavior has been observed when silica nanospheres were used as support for metallocene catalysts (work in preparation).[37]

TEM images of the PE/SN nanocomposites containing 1 and 5 wt % silica nanospheres are shown in Figure 6. Although the 1 wt % PE/SN nanocomposite has zones where the presence of silica nanospheres is not observed, the particles do not appear agglomerated. The image of the 5 wt % PE/SN nanocomposite clearly shows the increased silica nanospheres concentration. This nanocomposite has a greater degree of agglomeration of the silica nanoparticles.

## Mechanical properties

The mechanical properties of the nanocomposites are shown in Table II and Figure 7. The stress–strain curves display a sharp force maximum at low strain, corresponding to the yield point, which is associated with the reorientation and destruction of the lamella by a process of c-shear, and depends on the lamellar thickness and crystallinity. That point represents the transition from elastic to plastic deformation, and the peak in the stress–strain curve is the point at which plastic flow becomes dominant.[38] Beyond this point, there is a decrease in the force with a further increase in elongation. In all cases the behavior of the samples is typical of HDPE. Upon formation of the neck, the deformed region whitens due to void formation. Finally, a strain hardening is observed until the breaking point is reached.[39]

The elastic modulus and yield stress of neat PE in this study are higher than those produced with other catalytic systems in the literature.[39] Furthermore, an increase of 19–25% in Young's modulus is achieved in the nanocomposite samples. This effect is independent of the percentage of nanospheres used and can be attributed to the higher rigidity caused by the presence of silica nanospheres. The Young's modulus of the samples with 5 wt % of silica nanospheres is slightly less than that obtained in samples with 1 wt % of silica nanospheres. This is likely due to the aggregation of the silica nanospheres at higher concentrations. The polymers obtained with silica

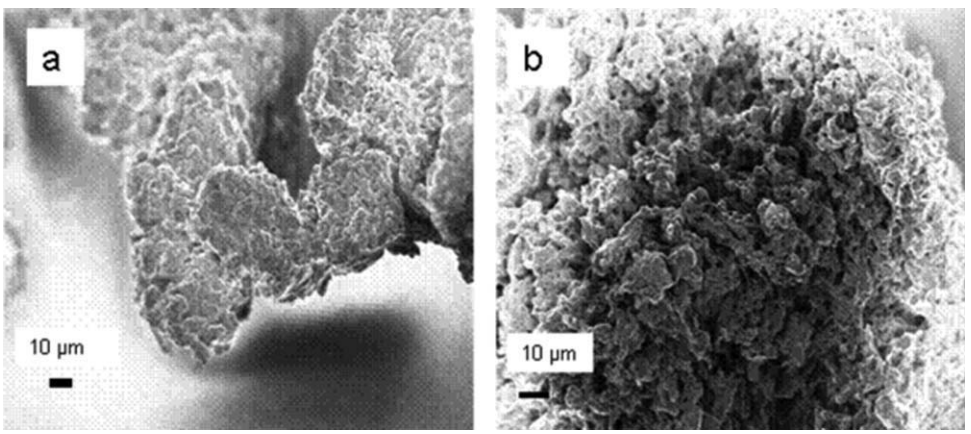


**Figure 5** SEM micrographs: (a) neat polymer and (b) PE/SN (1 wt %).

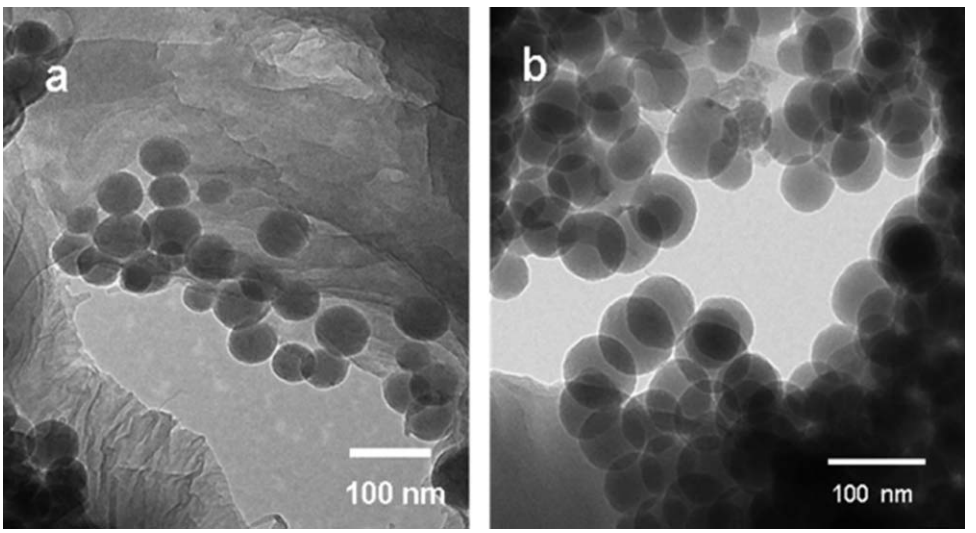


**Figure 6** TEM micrographs of PE/SN nanocomposite with (a) 1 wt % and (b) 5 wt % of SN.

nanospheres also have higher degrees of crystallinity than the neat polymer which could also be associated with the increase in Young's modulus. The elongation at rupture on the other hand does not decrease significantly compared to neat PE.

Microhardness measurements were made using the Vickers microindentation hardness test, a method that measures the resistance of a material to the plastic deformation produced by the impact of an indentor. The microhardness (MH) of polymers has been related to other mechanical properties (yield stress and Young's modulus in particular) by considering the roles that the crystalline, amorphous, and interfacial regions play in the deformation of a semicrystalline polymer.[40] This method is also capable of testing the surface mechanical properties of polymers as a function of processing conditions, heat treatment, microstructure, and other physical treatment.

The microhardness (MH) values of the different polymer samples are shown in Table II. In semicrystalline polymers, MH will depend on the content of crystalline and amorphous parts. The major contribution to the total value of MH is that of the crystalline phase.[38,41,42] These MH values show an increase with the incorporation of silica nanospheres. These results confirm the increased Young's modulus of the nanocomposites found through dynamometer measurements (Table II and Fig. 7).

Microhardness measurements at different points on the polymer matrix can be also used to monitor the degree of dispersion of the silica nanospheres. The variation of MH in nanocomposites with 5 wt % silica was somewhat greater than that observed in samples with 1 wt % silica and this can be attributed to the lower dispersion of silica nanospheres in the 5 wt % PE/SN nanocomposite.

### Dynamic-mechanical properties

The viscoelastic behavior of PE is strongly influenced by variables that affect the crystalline regions, such as crystallinity, lamellar thickness, and the interface.[43]

Plots of the storage ($E'$), loss modulus ($E''$), and loss tangent (tan δ) as a function of temperature at 3 Hz for linear PE and the PE/SN nanocomposite (1 and 5 wt % SN) are shown in Figure 8, and the storage modulus at room temperature and apparent activation energy are shown in Table III. The tan δ and loss modulus ($E''$) maximums show that two relaxations (α and γ) take place in the specimens. These are accompanied by a pronounced decrease of the storage modulus.

**TABLE II**
**Mechanical Parameters and Microhardess (MH) of Neat PE and its Composites, PE/SN, Analyzed at 25°C**

| Process | Silica Nanosphere content (%) | $E$ (MPa) | $\sigma_y$ (MPa) | $\varepsilon_{break}$ (%) | MH (MPa) |
|---|---|---|---|---|---|
| Neat PE | 0 | 610 ± 60 | 24 ± 2 | 305 ± 50 | 34 ± 1 |
| PE/SN nanocomposite | 1 | 780 ± 30 | 27 ± 1 | 290 ± 95 | 38 ± 0.9 |
| | 5 | 730 ± 50 | 25 ± 2 | 200 ± 60 | 40 ± 1.3 |

Young's modulus ($E$), yield stress, ($\sigma_y$), deformation at break ($\varepsilon_{break}$), microhardness (MH).

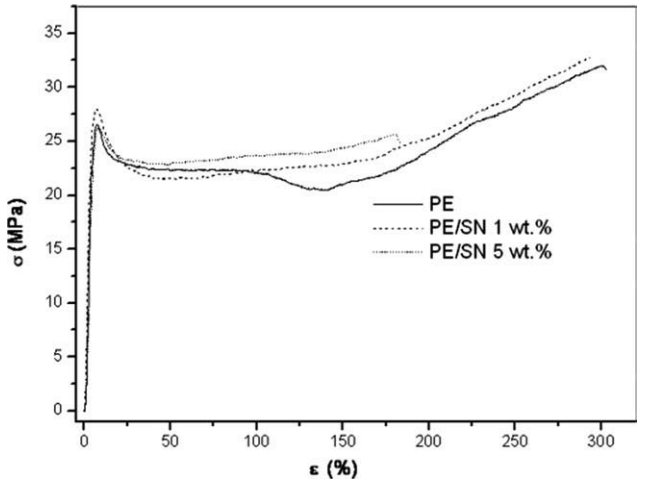


**Figure 7** Stress–strain curves for the PE/SN (Yield stress, $\sigma_y$, versus deformation at break, ε,).

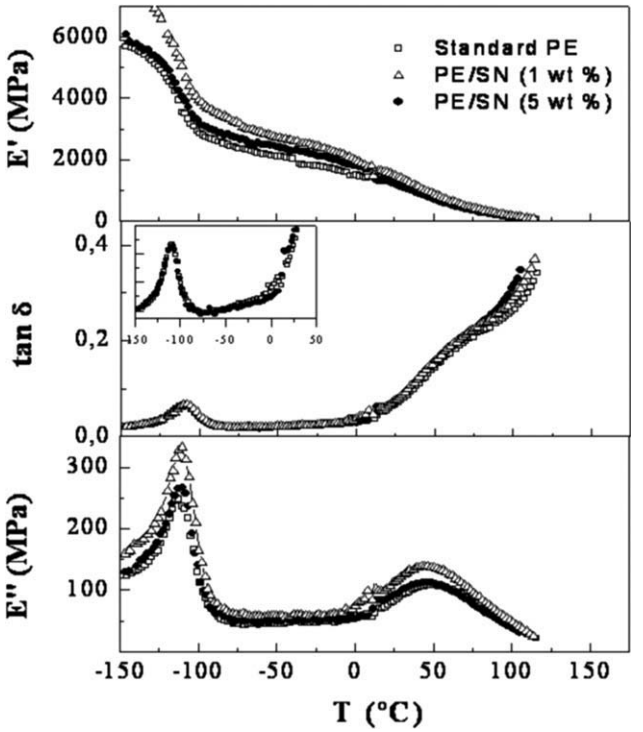


**Figure 8** Variation of the storage modulus ($E'$), loss tangent (tan δ), and loss modulus ($E''$) with temperature for neat PE and for PE/SN nanocomposites with 1 and 5 wt % of SN.

The α-relaxation has been assigned to reorientation of molecules within the crystals.[35] It has been reported[44] that there is a relation between crystal thickness and intensity of the α-relaxation, and that this process is affected by the chain mobility of the crystals. Therefore, chain mobility occurs at higher temperatures as crystallite thickness increases. In general, the position and intensity of the α-relaxation maximum have been related to crystal thickness and crystallinity level, respectively. In the present PE sample, the α relaxation appears centered at 49°C and in the PE/SN nanocomposites at 45°C (at 3 Hz in $E''$). The activation energy, $\Delta H$, calculated from $E''$ curves assuming a single process (see Table III), takes the values of 128, 123, and 124 kJ mol$^{-1}$ for PE and PE/SN nanocomposites (1 and 5 wt % of SN), respectively, all values are slightly lower than those of other metallocene PEs. On the other hand, the lower temperature in the nanocomposites is attributed to a narrow distribution of the crystals, and therefore lower activation energy is needed.

The α relaxation does not show a clear maximum in tan δ, the data sweeping up steeply towards the melting temperature of the polymer. These results are similar to those in other HDPEs and LLDPEs as a consequence of the larger crystal size present in PE.[45]

The γ-relaxation has been associated with a single relaxation process, predominantly of amorphous origin. This relaxation is typical of the joint movements of chains containing three or more methylene units in the main chain.[44] The γ relaxation appears at −113°C for neat PE and at −110°C for the PE/SN nanocomposites with 1 and 5 wt % of SN, in loss modulus maxima at 3 Hz. The γ-transition peak intensity increases for the PE/SN nanocomposite with 1 wt % of SN. This relaxation is attributed to the motions of the $CH_2$ units in the amorphous region. In this sense, the apparent activation energy increases with the SN content, as expected from the higher crystallinity.

On the other hand, there is no evidence in these samples of the β relaxation typical in LDPE, LLDPE, as well as in some samples of linear polyethylene.[46,47] Its molecular origin is related to the motion of chain units in the interfacial region[48,49] although some other authors have attributed this process to the glass transition. This relaxation process does not

**TABLE III**
**Viscoelastic Properties of PE/SN Nanocomposites: Storage Modulus ($E'$), at 25°C, Temperature and Apparent Activation Energies of the Relaxation α and γ (in $E''$ at 3 Hz)**

| Process | Silica nanosphere content (%) | $E'^{25°C}$ (MPa) | $T_\alpha$ (°C) | $T_\gamma$ (°C) | $\Delta H_\alpha$ (kJ mol$^{-1}$) | $\Delta H_\gamma$ (kJ mol$^{-1}$) |
|---|---|---|---|---|---|---|
| Neat PE | 0 | 1230 | 49 | −113 | 128 ± 5 | 98 ± 5 |
| PE/SN nanocomposite | 1 | 1490 | 45 | −110 | 123 ± 5 | 140 ± 10 |
| | 5 | 1270 | 45 | −111 | 124 ± 5 | 125 ± 15 |

take place in the homopolymer, nor in the nanocomposites, Figure 8. Its absence indicates that the interfacial content in all specimens is very low and not important. In other words, that there is good interaction between the matrix and the nanofiller.

The storage and loss modulus of the PE/SN nanocomposite (1 wt %) were higher than those of neat PE. It has been suggested that the increased storage modulus of a composite with $SiO_2$ can be due to the fact that the macromolecular chains at the interface are restricted by the surface of the filler, greatly limiting molecular motion.[6] As result of these changes, the storage modulus of the interface is higher than that of the free part.

In general, for polyethylene with 5 wt % of silica nanospheres the visoelastic properties did not significantly change, which can be due to the high degree of agglomeration of silica nanospheres. The behavior of the storage modulus at 25°C is similar to other mechanical properties (stress–strain deformation and microhardness).

## CONCLUSIONS

PE nanocomposites were prepared by *in situ* polymerization using silica nanospheres as filler. The polymerization activity of the metallocene catalyst increased slightly in the presence of 1 wt % nanospheres. The nanocomposites obtained with a few weight-percent of silica nanospheres (1–5 wt %) had a significant improvement (19–25%) in Young's modulus without significant decreases to the elongation at break with respect to neat polyethylene. Storage and loss modulus for the PE/SN nanocomposite (1 wt %) were higher than those of neat PE. The presence of silica nanospheres also improves the textural morphology of the polyethylene product. It is thought that the modification of the silica nanosphere surface would result in improved dispersion into the polymer matrix.

Special thanks are due to Professor Dr. Gerhard Wegner and Dr. Ingo Lieberwirth, of the Max Planck Institute for Polymer Research, Mainz, Germany, for providing the TEM equipment, and to Professor Jaime Retuert for his support during this research. Paula Z. thanks the Deutscher Akademischer Austauschdienst (DAAD) for a Ph.D. fellowship.

## References

1. Wang, Q.; Zhou, Z.; Song, L.; Xu, H.; Wang, L. J Polym Sci A Polym Chem 2004, 42, 38.
2. Hwu, J.; Jiang, G. J Appl Polym Sci 2005, 95, 1228.
3. Rong, M.; Zhang, M.; Pan, S.; Friedrich, K. J Appl Polym Sci 2004, 92, 1771.
4. Kawasumi, M.; Hasegawa, N.; Kato, M.; Usuki, A.; Okada, A. Macromolecules 1997, 30, 6333.
5. Xu, J.; Zhao, Y.; Wang, Q.; Fan, Z. Eur Polym Mater 2005, 41, 3011.
6. Kontuo, E.; Niaounakis, M. Polymer 2006, 47, 1267.
7. Moncada, E.; Quijada, R.; Retuert, J. Nanotechnology 2007, 18, 335606, 1.
8. García, M.; Zyl, W.; Cate, G.; Stouwdam, J.; Verweij, H.; Pimplaupure, M.; Weickert, G. Ind Eng Chem Res 2003, 42, 3750.
9. Kaminsky, W.; Funck, A. Macromol Symp 2007, 260, 1.
10. Chaichana, E.; Jongsomjit, B.; Praserthdam, P. Chem Eng Sci 2007, 62, 899.
11. Jongsomjit, B.; Panpranot, J.; Praserthdam, P. Mater Lett 2007, 61, 1376.
12. Kaminsky, W. J Polym Sci A Polym Chem 2004, 42, 3911.
13. Velilla, T.; Delgado, K.; Quijada, R.; Bianchini, D. J Polym Sci A Polym Chem 2007, 45, 5480.
14. Kuo-Tseng, Li.; Dai, C.; Kuo, C. Catal Commun 2007, 8, 1209.
15. Alexandre, M.; Dubois, P.; Sun, T.; Garces, M.; Jeronime, R. Polymer 2002, 43, 2123.
16. Lee, D.; Kim, H.; Yoon, K.; Min, K.; Seo, K.; Noh, S. Sci Technol Adv Mater 2005, 6, 457.
17. Zapata, P.; Quijada, R.; Covarrubia, C.; Moncada, E.; Retuert, J. J Appl Polym Sci 2009, 113, 2368.
18. Kim, K.; Taik, H. J Sol Gel Sci Technol 2002, 25, 183.
19. Dos santos, J. H. Z.; Krung, C.; Da Rosa, M.; Stedile, F.; Dupont, J.; Forte, M. J Mol Catal A Chem 1999, 139, 199.
20. Kristen, M. Topic Catal 1999, 7, 89.
21. Chien, J. Topic Catal 1999, 7, 23.
22. Kuo-Tseng, L.; Kuo, Y. J Appl Polym Sci 2006, 101, 2573.
23. Kaminsky, W.; Funck, A. Macromol Symp 2006, 239, 1.
24. Bianchi, D.; Chiarello, S.; Dos Santos, J. H. Z. Appl Catal A Gen 2004, 261, 57.
25. Pedro, C.; Carrillo-Hermosilla, F.; Alonso-Moreno, C.; Otero, A.; Antiñolo, A.; Sancho, J.; Villaseñor, E. J Mol Catal A Chem 2006, 258, 236.
26. Wei, L.; Tang, T.; Huang, B. J Polym Sci A Polym Chem 2004, 42, 941.
27. Gao, Y.; Choudhury, N.; Dutta, N.; Matisons, J.; Reading, M.; Delmotte, L. Chem Mater 2001, 13, 3644.
28. Lopez, T.; Asomoza, M.; Gómez, R. J Non Cryst Solids 1992, 147, 769.
29. Galland, G.; Seferin, M.; Gumaraes, R.; Rohrmann, J.; Stedile, F.; Dos Santos, J. H. Z. J Mol Catal A Chem 2002, 189, 233.
30. Bianchi, D.; Dos Santos, J. H. Z.; Uozumi, T.; Sano, T. J Mol Catal A Chem 2002, 185, 223.
31. Zechlin, J.; Hauschild, K.; Fink, G. Macromol Chem Phys 2000, 201, 597.
32. Simpício, L.; Gomes, F.; Soares, J.; Andrede, E.; Teixeira, S. J Mol Catal A Chem 2004, 216, 45.
33. Grieken, R.; Carreo, A.; Suarez, I.; Paredes, B. E. Polym J 2000, 43, 1267.
34. Osman, M.; Rupp, J.; Suter, U. Polymer 2005, 46, 1653.
35. Jordens, K.; Wilkes, G.; Janzen, J.; Rohlfing, D.; Welch, M. Polymer 2000, 41, 7175.
36. Kuo, S.; Huang, W.; Huang, S.; Kao, H.; Chang, F. Polymer 2003, 44, 7709.
37. Zapata, P.; Quijada, R.; Retuert, J. IUPAC Macro 2008. Study of Catalytic Activity of Ethylene Polymerization with Support Metallocene Catalysts on Nanospheres. Polymers at Frontiers of Science and Technology 2008, Taipei-Taiwan.
38. Benavente, R.; Pérez, E.; Quijada, R. J Polym Sci Polym Phys 2001, 39, 277.
39. Sacristán, J.; Benavente, R.; Pereña, J. M.; Pérez, E.; Bello, A.; Rojas, R.; Quijada, R.; Rabagliati, F. M. J Thermal Anal Calorim 1999, 58, 559.
40. Benavente, R.; Pérez, E.; Pereña, J.; Bello, A.; Ribeiro, M.; Portela, M. Eur Polym J 2000, 36, 879.

41. Encyclopedia of Polymer Science and Engineering; Wiley: New York, 1987; Vol. 7, p 614.
42. Lorenzo, V.; Pereña, J. M.; Fatou, J. M. G. Makromol Chem 1989, 172, 25.
43. Cerrada, M. L.; Benavente, R.; Pérez, E. J Mater Res 2001, 16, 1103.
44. Benavente, R.; Pérez, E.; Yazdani-Pedram, M.; Quijada, R. Polymer 2002, 43, 6821.
45. Mathews, G.; Ward, I.; Capaccio, G. J Polym Sci Polym Phys 1999, 37, 51.
46. Zamfirova, G.; Pereña, J. M.; Benavente, R.; Pérez, E.; Cerrada, M. L.; Nedkov, E. Polym J 2002, 34, 125.
47. Nitta, K.-N.; Tanaka, A. Polymer 2001, 42, 1219.
48. Popli, R.; Mandelkern, L. Polym Bull 1983, 9, 260.
49. Popli, R.; Glotin, M.; Mandelkern, L.; Benson, R. S. J Polym Sci Polym Phys 1984, 22, 407.